



Investigation of Materials for Boundary Layer Control in a Supersonic Wind Tunnel

Alexander C. Braafladt
The University of Minnesota, Minneapolis, Minnesota

John M. Lucero and Stefanie M. Hirt
Glenn Research Center, Cleveland, Ohio

NASA STI Program . . . in Profile

Since its founding, NASA has been dedicated to the advancement of aeronautics and space science. The NASA Scientific and Technical Information (STI) program plays a key part in helping NASA maintain this important role.

The NASA STI Program operates under the auspices of the Agency Chief Information Officer. It collects, organizes, provides for archiving, and disseminates NASA's STI. The NASA STI program provides access to the NASA Aeronautics and Space Database and its public interface, the NASA Technical Reports Server, thus providing one of the largest collections of aeronautical and space science STI in the world. Results are published in both non-NASA channels and by NASA in the NASA STI Report Series, which includes the following report types:

- **TECHNICAL PUBLICATION.** Reports of completed research or a major significant phase of research that present the results of NASA programs and include extensive data or theoretical analysis. Includes compilations of significant scientific and technical data and information deemed to be of continuing reference value. NASA counterpart of peer-reviewed formal professional papers but has less stringent limitations on manuscript length and extent of graphic presentations.
- **TECHNICAL MEMORANDUM.** Scientific and technical findings that are preliminary or of specialized interest, e.g., quick release reports, working papers, and bibliographies that contain minimal annotation. Does not contain extensive analysis.
- **CONTRACTOR REPORT.** Scientific and technical findings by NASA-sponsored contractors and grantees.

- **CONFERENCE PUBLICATION.** Collected papers from scientific and technical conferences, symposia, seminars, or other meetings sponsored or cosponsored by NASA.
- **SPECIAL PUBLICATION.** Scientific, technical, or historical information from NASA programs, projects, and missions, often concerned with subjects having substantial public interest.
- **TECHNICAL TRANSLATION.** English-language translations of foreign scientific and technical material pertinent to NASA's mission.

Specialized services also include creating custom thesauri, building customized databases, organizing and publishing research results.

For more information about the NASA STI program, see the following:

- Access the NASA STI program home page at <http://www.sti.nasa.gov>
- E-mail your question to help@sti.nasa.gov
- Fax your question to the NASA STI Information Desk at 443-757-5803
- Phone the NASA STI Information Desk at 443-757-5802
- Write to:
STI Information Desk
NASA Center for AeroSpace Information
7115 Standard Drive
Hanover, MD 21076-1320



Investigation of Materials for Boundary Layer Control in a Supersonic Wind Tunnel

Alexander C. Braafladt
The University of Minnesota, Minneapolis, Minnesota

John M. Lucero and Stefanie M. Hirt
Glenn Research Center, Cleveland, Ohio

Prepared for
The Joint Machinery Failure Prevention Technology (MFPT) 2013 and 59th International Instrumentation Symposium (IIS)
cosponsored by the Society for Machinery Failure Prevention Technology and the International Society of Automation
Cleveland, Ohio, May 13–17, 2013

National Aeronautics and
Space Administration

Glenn Research Center
Cleveland, Ohio 44135

Trade names and trademarks are used in this report for identification only. Their usage does not constitute an official endorsement, either expressed or implied, by the National Aeronautics and Space Administration.

Level of Review: This material has been technically reviewed by technical management.

Available from

NASA Center for Aerospace Information
7115 Standard Drive
Hanover, MD 21076-1320

National Technical Information Service
5301 Shawnee Road
Alexandria, VA 22312

Available electronically at <http://www.sti.nasa.gov>

Investigation of Materials for Boundary Layer Control in a Supersonic Wind Tunnel

Alexander C. Braafladt,* John M. Lucero, and Stefanie M. Hirt
National Aeronautics and Space Administration
Glenn Research Center
Cleveland, Ohio 44135

Abstract

During operation of the NASA Glenn Research Center 15- by 15-Centimeter Supersonic Wind Tunnel (SWT), a significant, undesirable corner flow separation is created by the three-dimensional interaction of the wall and floor boundary layers in the tunnel corners following an oblique-shock/boundary-layer interaction. A method to minimize this effect was conceived by connecting the wall and floor boundary layers with a radius of curvature in the corners. The results and observations of a trade study to determine the effectiveness of candidate materials for creating the radius of curvature in the SWT are presented. The experiments in the study focus on the formation of corner fillets of four different radii of curvature, 6.35 mm (0.25 in.), 9.525 mm (0.375 in.), 12.7 mm (0.5 in.), and 15.875 mm (0.625 in.), based on the observed boundary layer thickness of 11.43 mm (0.45 in.). Tests were performed on ten candidate materials to determine shrinkage, surface roughness, cure time, ease of application and removal, adhesion, eccentricity, formability, and repeatability. Of the ten materials, the four materials which exhibited characteristics most promising for effective use were the heavy body and regular type dental impression materials, the basic sculpting epoxy, and the polyurethane sealant. Of these, the particular material which was most effective, the heavy body dental impression material, was tested in the SWT in Mach 2 flow, and was observed to satisfy all requirements for use in creating the corner fillets in the upcoming experiments on shock-wave/boundary-layer interaction.

Introduction

In the design and creation of next-generation supersonic aircraft, engine performance is a critical factor. Supersonic inlets are thus designed to efficiently decelerate and compress the airflow to the engine in order to maximize performance. At the supersonic flight regimes of next-generation aircraft, mixed compression inlets are required for efficient flight. Mixed compression inlets decelerate and compress flow through the use of both external oblique shocks and internal reflected oblique shocks followed by an internal terminal normal shock, an example of which is shown in Figure 1. This system of shock waves, while important for efficient pressure recovery at the engine, has the negative effect of thickening, and possibly separating, the boundary layer where the shock waves impact the walls of the inlet and interact with the boundary layer. Here, pressure recovery is defined as the ratio of the total pressure at the engine face to that at the inlet entrance (Ref. 1). The boundary layer is defined as the region of flow near to the inlet walls in which friction is significant. This region conventionally has a width equal to the height above the surface at which the value of velocity is 99 percent of the value far away from the wall.

*NASA Glenn Research Center, summer intern from University of Minnesota.

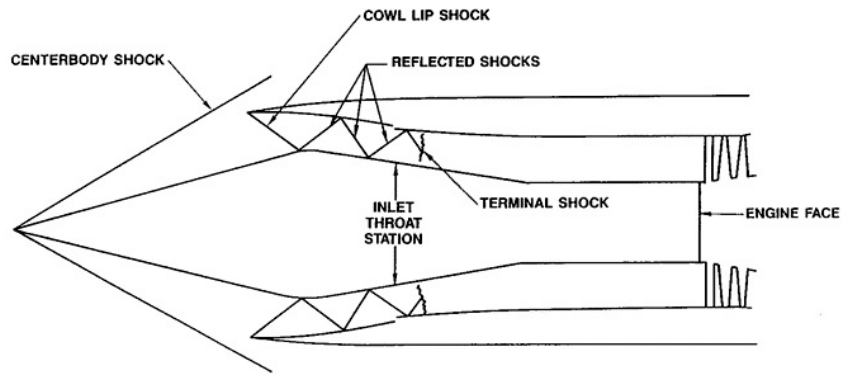


Figure 1.—A sketch of the SR-71 inlet and mixed compression shock structure (Ref. 8).

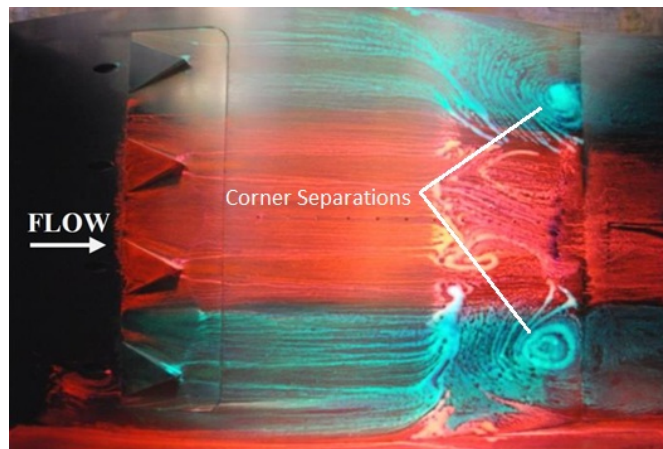


Figure 2.—Oil flow visualization showing significant corner separations in hybrid flow control testing at the NASA 15- by 15-Centimeter SWT (Ref. 14).

Separation of the boundary layer occurs when the flow detaches from the wall, and flow moving in the opposite direction of the free stream is observed in the lower boundary layer (Ref. 2). The result of the thickening of the boundary layer, along with possible boundary layer separation, is flow distortion, or nonuniformity in the total pressure profile of the flow at the engine face, causing a reduction in engine performance. In order to reduce this problem caused by the shock-wave/boundary-layer interactions (SBLI), boundary layer bleed is conventionally used as a method of flow control (Ref. 3). Boundary layer bleed is the removal of low momentum flow from near the wall, decreasing the boundary layer thickness, and therefore reducing flow distortion to the engine. However, bleed results in the drawbacks of increased drag, an increase in required inlet size, and the required inclusion of complex ducting systems. These drawbacks lead to a less efficient and more complex engine. To address these disadvantages, recent research has been conducted using methods of passive flow control intended to reduce the need for bleed in supersonic inlets (Refs. 4 to 7).

The main focus of this passive flow control research has been on vortex generators, such as micro-ramps and micro-vanes. These passive flow control devices are designed to improve boundary layer health (i.e., reduce distortion) by using vortices to mix high momentum flow from the upper boundary layer with low momentum flow in the lower boundary layer. These passive flow control devices have been tested for application in both axisymmetric and rectangular, two-dimensional inlets (Ref. 9). In the research on rectangular inlets, observations of significant corner separation have been made (Refs. 10 to 14). An example of such an observation is shown in Figure 2. Observations of rectangular duct SBLI three-dimensionality, in combination with a decrease in centerline boundary layer health when corner boundary layer health is improved (and vice versa), have also recently been made (Ref. 13). In response

to these observations, recent efforts have been made to further understand these interactions, along with the application of, and differences between, traditional corner bleed and possible passive corner flow control (Refs. 10, 13, 15, and 16).

As a continuation of this research experiments are planned at the NASA Glenn Research Center 15- by 15-Centimeter SWT to parameterize the effects of corner fillet flow control on an oblique SBLI by varying the radius of curvature, the total length, and the length of the tapered section at the upstream end of the fillets. Traditional inserts used in supersonic wind tunnels are machined out of stainless steel so as to keep the same surface properties as the stainless steel SWT surface. For the planned corner flow control experiments, machining the fillets out of stainless steel poses a problem. With the small size of the fillets radii of curvature (6.35, 9.525, 12.7, and 15.875 mm), combined with lengths of 25.4 to 55.88 cm (10 to 22 in.), the extremely thin tapered sections, and the extremely thin edges required to lie flush to the wind tunnel walls, fillets machined out of stainless steel would be extremely difficult to handle. Still further, if the radii of curvature were fabricated directly onto new removable wall sections, the costs of the experiments would increase significantly, well past available funding. Based on these problems, an approach using polymer/adhesive materials to form removable, one-time-use fillets was proposed. This method is required to produce a fillet from some material that can stay adhered in supersonic flow, while still offering surface roughness comparable to the stainless steel tunnel surface, shown in Figure 3 and having a measured value of $R_a = 0.2427 \mu\text{m}$. Additionally, the material must not damage the wind tunnel, must be able to be formed into a fillet in a timely manner, and must form into surface profiles which are as precise as possible while still retaining accuracy. From these requirements, ten readily available candidate materials were chosen to be the focus of a trade study into which material is best suited for use in the wind tunnel. The study includes both preliminary tests in aluminum angle stock corners along with tests in the SWT stainless steel corners. The ten materials are listed in Table 1 along with available information on what polymer they are composed of.

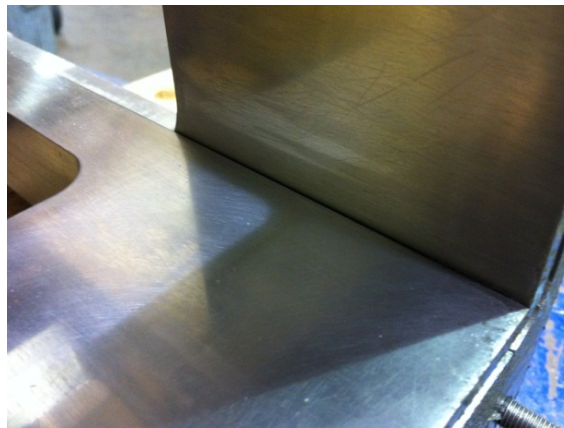


Figure 3.—NASA Glenn 15- by 15-Centimeter SWT test section corner.

TABLE 1.—MATERIAL NAMES AND POLYMER TYPES

Material type	Composition
Polyurethane sealant	Polyurethane
Heavy body dental impression material	Vinyl polysiloxane
Regular type dental impression material	Vinyl polysiloxane
Polyester filler paste	Polyester
Silicate cement	N/A
Resin/solvent based sealant	N/A
Silicone adhesive sealant	Silicone
Vinyl adhesive caulk	Vinyl acetate homopolymer
Spackling paste	Vinyl acetate latex polymer
Basic sculpting epoxy	N/A

Technical Approach

The tests of the ten candidate materials (Table 2 with commercial product names) were performed using samples prepared in 1 in. width aluminum angle stock pieces of approximately 2 in. in length, as shown in Figure 4. The aluminum angle stock was used as a readily available approximation of the stainless steel surface in the wind tunnel (Fig. 3). The angle stock pieces were smoothed, buffed, and cleaned to simulate the wind tunnel corner surface. Roughness testing, as described below, determined the aluminum to have a resultant average roughness (R_a) of 2.104 μm as compared to 0.2427 μm for the finished stainless steel surface in the wind tunnel. This difference between the surfaces was determined to be acceptable for initial qualitative testing, as the tests in the wind tunnel include application of material to the wind tunnel surface, and the initial tests were primarily designed to select the best of the candidate materials, especially eliminating materials that may result in damage to the wind tunnel.

Each candidate material was first extruded onto four different aluminum corners, and a fillet of the material was formed using Teflon rods with diameters of 12.7 mm (0.5 in.), 19.05 mm (0.75 in.), 25.4 mm (1.0 in.), and 31.75 mm (1.25 in.). The method for formation was, when possible, pressure directly into the corner (as seen in Fig. 5) with the Teflon rods, followed by lifting the rod off the corner either before or after material curing. In cases where the material pulls away with the Teflon rod, or would cure to the rod if allowed to, the fillets were formed either by inserting a plastic barrier (Fig. 6) between the rod and material that the material would not adhere to (and could be removed before or after curing), or by scraping the end of the rod lengthwise along the corner, pushing off excess material and leaving a fillet behind. Qualitative observations of the process to assess the ease of application and formability of the material were recorded. Additionally, for the materials that performed best in roughness testing (as described below), formation of the fillet was also conducted with a plastic 1 in. diameter rod to reduce surface roughness and characterize the effect of the roughness of the Teflon rods on the samples. The full test matrix for all samples is given in Table 3.

TABLE 2.—LIST OF CANDIDATE MATERIALS

Material type	Product name
Polyurethane sealant	Geocel 3300 Professional Grade Polyurethane Sealant
Vinyl polysiloxane dental impression material	GC America Examix NDS Heavy Body
Vinyl polysiloxane dental impression material	GC America Examix NDS Regular Type
Polyester filler paste	PTM&W Poly Filler HT
Silicate cement	Red Devil Fireplace and Stove Silicate Cement
Resin/solvent based sealant	Red Devil Zip-A-Way Removable Weather Stripping
Silicone adhesive sealant	Loctite Superflex Clear RTV Silicone Adhesive Sealant
Vinyl adhesive caulk	Phenoseal Does it All Vinyl Adhesive Caulk
Spackling paste	Dap/Bondex Spackling Paste
Basic sculpting epoxy	GF9/Kneadate Green Stuff Basic Epoxy

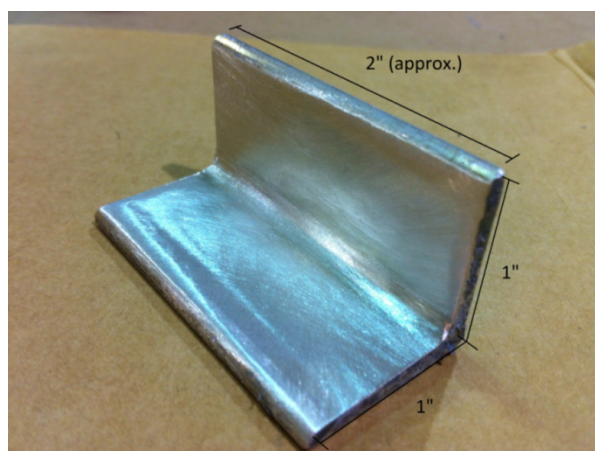


Figure 4.—A piece of aluminum angle stock.



Figure 5.—Fillet formation for the regular type dental impression material using the 3/4 in. diameter Teflon rod.



Figure 6.—Plastic film was used with some materials to allow the formation of a fillet with the Teflon rod.

TABLE 3.—TEST MATRIX

Sample number's	Material type	Plastic film	Teflon/plastic rod	Form fillet by scraping excess away	Spray paint	Zygo, mm
1 to 4	Spackling paste		T	X	X	9.525
5 to 8	Silicone adhesive sealant		T	X	X	9.525
9 to 12	Vinyl adhesive caulk		T		X	9.525
13 to 16	Silicate cement		T		X	9.525
17 to 20	Basic epoxy	X	T			9.525
21 to 24	Regular type dental impression		T			9.525
25 to 28	Heavy body dental impression		T			9.525
29 to 32	Polyurethane sealant		T	X		9.525
33 to 36	Resin/solvent based sealant		T	X	X	9.525
37 to 40	Polyester filler paste		T	X	X	9.525
41	Regular type dental impression		P			12.7
42 to 46	Heavy body dental impression		P			12.7
47 to 51	Polyurethane sealant		P	X	X	12.7

Following the formation of the fillet in the aluminum angle stock pieces, the samples were allowed to cure for the shortest of either the listed cure time or 16 hr. The 16 hr period was selected based on the desire during the aerodynamic testing of the fillets to have the material applied to the tunnel corners at the end of a work day, and testing occur in the tunnel the following morning. After this initial cure time, observations of the cured material were recorded to assess the shrinkage, surface roughness, and the overnight curability of the materials. The 16 hr cure time differed from the listed cure time for a number of materials, and qualitative observations were also recorded after the full listed cure time for these materials. This was done in order to get a full assessment of suitability for use in the wind tunnel, including any length of cure time.

After fully curing, the 9.525 mm (3/4 in.) samples (12.7 mm samples with the plastic rod application process) were profiled using a scanning white light interferometer (SWLI) using MetroPro 8 software, as shown in Figure 7 and calibrated annually (most recently on October 4th, 2012). This allowed measurements of the average surface roughness in micrometers and a profile of the surface to be output as a set of data points. The process for obtaining these measurements involved “stitches” (a combination of a series of individual measurements) across the width of the samples in three places as shown in Figure 8. For some samples an acrylic spray paint was used to allow the SWLI to reflect enough light off the material for measurements, and these samples are indicated in Table 3. The SWLI calculates the R_a values as the arithmetic average deviation from the mean value along the linear, streamwise direction, as given in Equation (1). The R_a values measured by the SWLI in μm are accurate to within a noise level of $\pm 0.020 \mu\text{m}$ (Ref. 17).

$$R_a = \frac{y_1 + y_2 + y_3 + \dots + y_N}{N} \quad (1)$$



Figure 7.—Zygo NV5032 scanning white light interferometer.

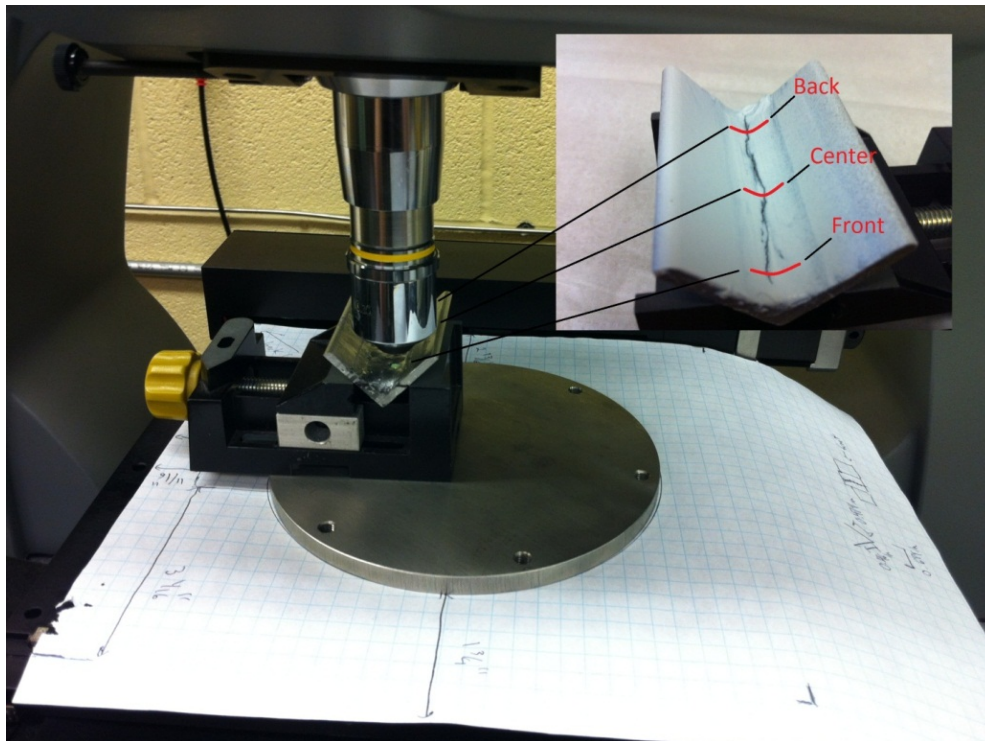


Figure 8.—The locations of the three measurements made by the Zygo NV5032 SWLI.

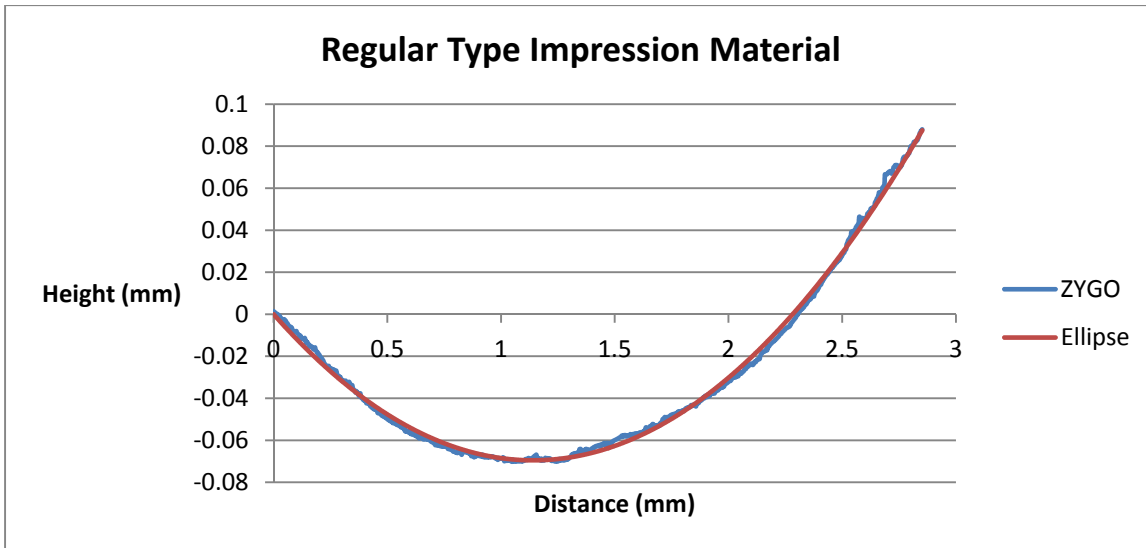


Figure 9.—Curve fit of an ellipse to the data from the SWLI for the regular type impression material applied with the Teflon rod.

Using the surface profile data points, Microsoft Excel (Microsoft Corporation) was used to determine the eccentricity of the samples at each stitch. This was done by curve fitting an ellipse to the profile data using the GRG Nonlinear Solver Excel Add-In to minimize the square root of the sum of the error between the data points output from the SWLI and the ellipse. An example of an ellipse fit to the profile data is included in Figure 9. In order to compare repeatability, measurements of eccentricity were also compared statistically.

Following these preliminary tests, the material which preformed best (the heavy body dental impression material as discussed below) was tested in a stainless steel corner and qualitatively compared to the previous samples in the aluminum corners. This material was then formed in the SWT corner and observed for 2 hr in Mach 2 flow, with Reynolds numbers from approximately 13 million per meter (planned test conditions) to 26 million per meter (4 to 8 million per foot).

Results and Discussion

The set of ten candidate materials, in order to determine those most suitable for use as corner flow control (in the form of a corner fillet) in the supersonic wind tunnel, were differentiated based on qualitative criteria, surface roughness and eccentricity measurements, and repeatability calculations. The tabulated results of the surface roughness and eccentricity measurements along with repeatability calculations are given in Table 4, and the qualitative results are given in Table 5. The qualitative results are assessed on a scale of 1 to 5 where 5 indicates excellent performance with respect to effective use in the wind tunnel, and 1 indicates that use in the wind tunnel would be impossible or damaging to the tunnel.

Surface Roughness

The surface roughness measurements made with the SWLI are given in Table 4 for each material. These values are of the average roughness parameter R_a in micrometers, sampled from the SWLI data in the lengthwise, or streamwise, direction. These R_a values are the mean combination of 7 to 10 R_a samples from each of the three locations where measurements were made with the SWLI on each material sample (Fig. 8). From Table 4 the sample with the lowest R_a value from the initial set of 41 samples is the regular type dental impression material sample created using the plastic 1 in. rod with a value of $R_a = 0.8790 \mu\text{m}$. During measurements for repeatability (as described below), surface roughness values were also

measured for heavy body dental impression material samples formed using the plastic rod, with an even lower mean value of $R_a = 0.2781 \mu\text{m}$. Comparatively, the average roughness of a previous stainless steel wind tunnel hardware insert (Fig. 10) is $0.2427 \mu\text{m}$. The values of the best samples are very near to the stainless steel hardware insert surface roughness, and therefore show no indication that surface roughness will be a parameter to prevent use in the SWT for the dental impression materials. However, as seen in looking at the edges of the radii in Figures 12 and 18 in Appendix A, the possibility of developing macroscopic roughness if the thin material at the edges cannot stay adhered to the tunnel wall does exist.

TABLE 4.—QUANTITATIVE FIGURES OF MERIT

Material type	R_a (μm) ± 0.020	Cure time	Eccentricity	Repeatability
Heavy body dental impression (plastic rod)	0.2781	5 min	0.1942	0.02627
Regular type dental impression (plastic rod)	0.8790	5 min	0.0582	-----
Heavy body dental impression	1.1533	5 min	0.2668	-----
Regular type dental impression	1.3310	5 min	0.2212	-----
Basic epoxy (plastic film)	1.9873	5 to 24 hr	0.3710	-----
Polyurethane sealant	1.9473	3 to 48 hr	0.6471	0.1354
Silicone adhesive sealant	3.1523	24 hr	0.2605	-----
Resin/solvent based sealant	1.8353	3 to 24 hr	0.8652	-----
Spackling paste	7.0660	1 to 5 hr	0.8087	-----
Silicate cement	6.9183	3 to 4 hr	0.7917	-----
Vinyl adhesive caulk	10.9183	12 to 48 hr	0.7349	-----
Polyester filler paste	6.7817	25 min	0.9587	-----

TABLE 5.—QUALITATIVE FIGURES OF MERIT

Material type	Shrinkage	Flow during application	Formability	Ease of removal	Adhesion to surface
Dental impression (plastic rod)	5	5	5	5	3
Heavy body dental impression	5	5	5	5	3
Regular type dental impression	5	5	5	5	3
Basic epoxy (plastic film)	5	4	4	3	4
Polyurethane sealant	5	4	2	3	5
Silicone adhesive sealant	5	2	2	2	5
Resin/solvent based sealant	3	4	2	5	2
Spackling paste	1	3	2	5	5
Silicate cement	1	4	2	4	5
Vinyl adhesive caulk	1	1	2	2	4
Polyester filler paste	5	3	2	1	5



Figure 10.—Stainless steel wind tunnel hardware used in previous experiments in the 15- by 15-Centimeter SWT.

A second group of materials with values of R_a ranging from 1.0 to 3.5 μm passes a visual test of acceptability for secondary use in the tunnel dependent on possible future in-tunnel tests. The remaining materials: polyester filler paste, silicate cement, spackling paste, and vinyl adhesive caulk; all have macroscopic textures which, in combination with poor R_a values, eliminate them from use in the SWT as radii of curvature for the planned corner flow experiments.

In the testing of the heavy body dental impression material (the best material after the preliminary tests) in the SWT, the application process was consistent to that of the samples in the aluminum angle stock, and resulted in a surface consistent to the surface of the samples in the aluminum corner samples. In tunnel conditions matching those of the planned corner flow testing, the edges of the radius did not fray or lift from the surface, resulting in no surface roughness problems. However, careful formation of radii is still necessary, as problems with the edges could still develop as different radius lengths and tapered sections are investigated.

Cure Time

For the ten materials tested, the suitability of the cure time for each material is based on the listed value, and on a 16 hr time period that is the length required for testing to be done on consecutive days. For many of the materials the 16 hr cure time is not attainable, as in testing they had not cured enough after 16 hr for use in the wind tunnel. This group included all the materials except for the dental impression materials, the polyester filler paste, the spackling paste, and the silicate cement. This Figure of Merit, while important, is flexible in that if the materials that satisfy the other requirements take longer than 16 hr to cure, it would be possible to use those materials, even though it would extend testing time for the flow control experiments. Be that as it may, as the best materials in most of the other Figures of Merit, the two dental impression materials, satisfy the 16 hr cure time requirement by a large margin, this material property is secondary with respect to the others.

In addition to the importance of cure times which allow testing on consecutive days, cure times which may be too short also are important. They are very important, as the ability to form the correct fillet, including tapered sections upstream, before the material cures enough to cause workability issues, is necessary for the success of the planned corner flow testing. The dental impression materials are the only materials to have cure times short enough (5 min) to possibly affect the quality of the fillet shape, and for these two materials the cure time has been long enough to form the fillet in all preliminary testing, including the formation of a test radius in the SWT. However, in the corner flow experiments, where full length fillets including tapered sections are required, the process might need to be broken into sections to be cured independently, and if necessary other application methods might need to be considered.

Eccentricity

The eccentricity of each fillet sample was determined by curve fitting an ellipse to raw surface profile data points. The average values of the fillet eccentricities are given in Table 4 and also are ranked from lowest to highest in Table 8 in Appendix B. For the flow control experiments, the objectives for the eccentricity of the fillets are first, consistent, repeatable values of eccentricity, and second, values of eccentricity as close to zero (circular) as possible. The repeatability of eccentricity is discussed below in the repeatability section. In terms of forming a radius as close to zero eccentricity as possible, the regular type dental impression material applied with the plastic rod resulted in the lowest average value of 0.0582. This value is very near to a circular, zero eccentricity ellipse. The curve fit of the ellipse to the data points from the SWLI is included in Figure 11. This value of eccentricity is more than adequate for the purposes of the corner flow experiments as the fillet profile is almost indistinguishable from a perfectly circular section.

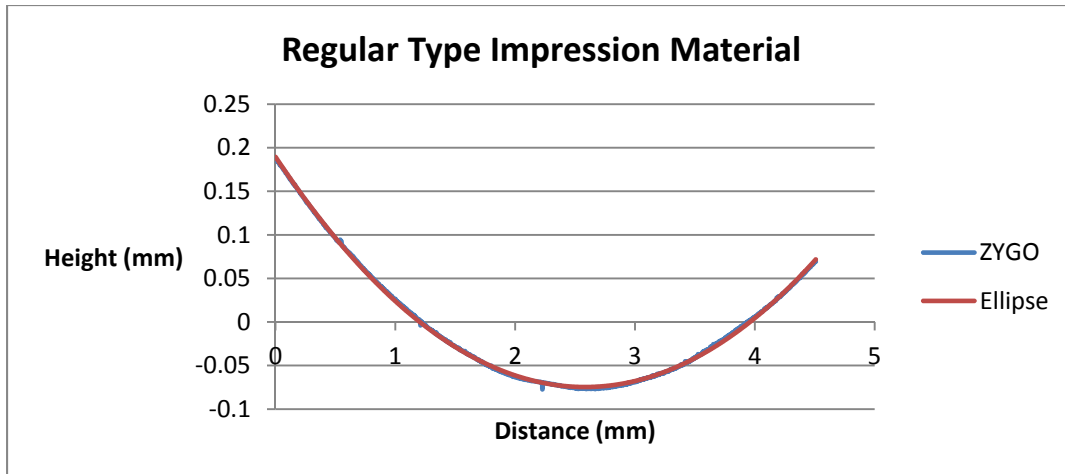


Figure 11.—Curve fit of an ellipse to the profile data obtained from the SWLI for the regular type impression material applied with the plastic rod.

For the other materials, the eccentricity as given in Table 4 can be referenced with the formation method for the material as given in Table 3. In comparison between materials for which the fillet was formed by scraping excess material away and those for which the fillet was formed by direct pressure and removal, it can be seen that the application method may have an effect on the eccentricity of the samples. This is further evidenced by examining conic sections and the fact that as a circle is rotated perpendicularly (in the same way that a plane is rotated through a cone to change a circular section to an elliptical section) eccentricity is introduced. This is the same change created by the angle at which the fillet is formed with the rods. For these materials, use is then dependent on whether the error in repeatability of the eccentricity is acceptable, although if necessary, a new application method may need to be investigated.

Repeatability

Using the qualitative observations made for each material, along with surface roughness measurements and raw values of eccentricity, a characterization of the repeatability of eccentricity for the best performing materials was determined. From the materials that did not receive a 1 out of 5 for any qualitative category, the heavy body dental impression material and polyurethane sealant were chosen for additional SWLI measurements designed to determine and compare repeatability. These materials were chosen so as to compare the application method in which the rod is pressed down into the aluminum angle stock to create the radius of curvature (heavy body dental impression material), with that in which the rod is used to scrape away the radius from the aluminum corner (polyurethane sealant). They were also chosen as the heavy body dental impression material can be removed relatively easily while the polyurethane sealant is much more difficult to remove.

The surface profiles output by the SWLI were qualitatively different. The profiles of the polyurethane sealant were observed to be much less consistent including macroscopic “bumps” where lines had formed along the length of the sample because of the application method, while those of the heavy body dental impression material were smooth and uniform. Visual observations of the polyurethane sealant without the SWLI also confirm the existence of lengthwise “bumps,” and other macroscopic imperfections of the surface caused by the application method, and this can be seen in comparing Figures 12 and 16 in Appendix A.

To compare the repeatability of the eccentricity of the two materials, eccentricity samples were again taken at three points along each of five samples of each material (as in Fig. 8), as described above in the eccentricity section. However, two different values of eccentricity were output for each “stitch” instead of 1, and 30 total values of eccentricity were obtained from five samples of each of the heavy body

impression material and polyurethane sealant. From these two sets of eccentricity values, a value of error between the profile output by the SWLI and a circle with zero eccentricity was defined, and is given in Equation (2). In this equation the two y values are, as indicated, the value of y position for both a circle (eccentricity of zero) and for the SWLI data point, both of which are at each x position from the data set, and also the circle is centered at the point of minimum error. In addition, N_y is the total number of data points output by the SWLI.

$$\text{error} = \frac{\sqrt{\sum_{i=1}^{N_y} (y_{\text{circle}} - y_{\text{SWLI}})^2}}{N_y} \quad (2)$$

This value of error was calculated for each surface profile of both the heavy body dental impression material and the polyurethane sealant. Outliers from each set were identified using the modified Thompson τ technique, and discarded (Ref. 18). As these sets are of the error between the measured surface profile and ellipses of zero eccentricity, a lower mean value indicates a material with profiles closer to circular, and, the focus of this section, a lower standard deviation indicates repeatability of eccentricity. The standard deviation of error for the heavy body dental impression material is 0.02627. For the polyurethane sealant the value is 0.1354, 5.15 times larger. This gives a clear indication not only that the heavy body dental impression samples are much more repeatable than the polyurethane sealant samples, but also that the method in which excess material is scraped off the aluminum corner with the plastic/Teflon rod is much less repeatable than direct formation of the radius of curvature (which is only possible for materials that do not stick to the rods and is indicated in Table 3).

Shrinkage

The shrinkage of the fillets after curing was assessed by post-cure qualitative observations of the four samples of each material. Most of the materials displayed no visual indication of shrinkage, although deviation in eccentricity from zero as given above may be due, in part, to shrinkage not easily visually apparent. The materials which exhibited visible shrinking or expanding during curing are the resin/solvent based sealant, the spackling paste, the silicate cement, and the vinyl adhesive caulk. The spackling paste and vinyl adhesive caulk both developed cracks as a result of shrinkage. For the resin/solvent based sealant, shrinking was observed visually and may be apparent in the large value of eccentricity as in Table 4, again however, the method required for forming the fillet may have affected this value of eccentricity to a degree. The silicate cement, which required heat to cure, expanded throughout curing, resulting in a surface profile which is nearly horizontally linear, along with an uneven macroscopic surface texture where some areas expanded more than others. Overall, the materials which developed cracks, and the silicate cement which expanded, cannot be used to create the fillet in the wind tunnel because these large shrinkage (or expansion) problems would create radii of curvature which are not precise or accurate for testing.

Flow During Application

The process of applying the different materials to the tunnel corners is an important parameter for determining which materials can be used in the wind tunnel. This process is divided into two parts for explicit definition: flow during application and formability. Formability is discussed in the next section. The flow during application was assessed qualitatively and is given with the other qualitative observations in Table 5. This Figure of Merit is based on the ease of applying the materials to the corner before forming the radius of curvature. Here, materials that are very difficult to handle, difficult to place into the corner, or require extensive personal protective equipment, fall lower on the 1 to 5 scale. These qualitative observations, while important, are also flexible in that they are dependent on the specific

packaging of the material and on the tools available for use. Most of the materials were similar overall in terms of flow during application with no observations indicating that use would be overly difficult in the wind tunnel. The only two materials to exhibit properties which make their use impossible or very difficult are the silicone adhesive sealant and the vinyl adhesive caulk. The vinyl adhesive caulk is impossible for use in the SWT in terms of this parameter as it has a very high viscosity and tends to have more cohesion than adhesion. The silicone adhesive is very difficult to apply as it is much more like glue than a sealant, and sticks to any tools used to apply it, pulling away from the corner.

The application of the best material (after preliminary tests the heavy body dental impression material) to the stainless steel SWT corner was identical to formation in the aluminum corner in terms of flow during application.

Formability

The formability of the materials was again qualitatively assessed on a scale of 1 to 5, where 1 indicates that creating the radii of curvature using the methods described above was impossible, and 5 indicates that it was simple and easy. The observations for each individual material are given in Table 5. The two dental impression materials were by far the easiest to form a radius of curvature with. After those two materials the basic sculpting epoxy is the only other material that did not have major problems with formability. The remaining materials were much more difficult to form. Of the materials, those which are indicated in Table 3 as formed using the method of scraping excess material away from the corner would require investigations of new application methods for use in the SWT. The vinyl adhesive caulk and the silicate cement, however, both had problems with formability which, through the observations of these tests, indicate that finding a method to create radii of curvature would be extremely difficult.

In formation of test radii in the stainless steel SWT corner, formability is only limited by access to the corners of the tunnel. The material tested in the SWT corner, the heavy body dental impression material was determined to be acceptable in terms of the formability of test radii; however, in formation of full lengths with tapered sections, the process for formation may need to be practiced or adjusted for best performance.

Ease of Removal

Most important for suitable use in the wind tunnel is the ease of removal for each material. This Figure of Merit was tested during removal of samples from the aluminum angle stock corners. The qualitative observations are included with the others in Table 5, where 1 indicates that removing the material from the corner would result in damage to the tunnel, and 5 indicates that removal is simple and quick. Most of the materials did not result in damage to the aluminum angle iron when removed, but the different methods required to do this did result in tedious or time consuming processes for some, and this is also reflected in the assessment value included in Table 5. The dental impression materials and the resin/solvent based sealant were the easiest to remove and therefore promising for using in the SWT, but must also be able to stay adhered to the wall in supersonic flow as described below.

The heavy body dental impression material was applied in the SWT stainless steel corner. The ease of removal was very similar between the stainless steel and the aluminum corners, although the limitation on accessibility in the wind tunnel did increase the difficulty slightly.

Adhesion to Surface

The adhesion of each material to the corner of the aluminum angle stock is approximated by the process of removing it either by hand or with tools, and the results are tabulated results in Table 5. These results are approximations in that they are purely qualitative observations intended to allow comparisons between the materials before they were tested in the wind tunnel. The two dental impression materials

were the best performing materials in terms of the other parameters, and as such, were selected for a possible test of adhesion in the SWT at Mach 2.0. Specifically, although the two are very similar, the heavy body material was chosen for testing, as it was observed to be qualitatively slightly more adhesive than the regular type dental impression material because of a higher rigidity. With no flow the heavy body impression material was tested in the wind tunnel corner, and was observed to have a similar, if slightly less strong, adhesion to the stainless steel wall in comparison to the aluminum angle stock corner. Following that test, the heavy body material was tested in Mach 2 flow for 2 hr at a Reynolds number of 13 million per meter followed by approximately a 1/2 hr at Reynolds numbers close to 26 million per meter. The material stayed adhered through all tests, and showed no indications of edges lifting or any areas having loosened from the surface of the tunnel.

Conclusion

In summary, a trade study was performed to determine the effectiveness of a set of materials for use in creating radii of curvature in SWT corners. The trade study included initial qualitative observations of shrinkage, ease of application and removal, formability, and adhesion, along with quantitative measurements of surface roughness, eccentricity, and repeatability.

The result of these initial tests was the selection of the regular type and heavy body dental impression materials, the basic sculpting epoxy, and the polyurethane sealant as candidates for possible use in the SWT (with all materials sorted by choice in Table 6 in Appendix B). This selection follows from comparing the materials using the parameters that were deemed to be most important: ease of removal, repeatability, formability, surface roughness, and eccentricity. The importance of these Figures of Merit is based on the need to prevent any possible damage to the wind tunnel, replicate the SWT surface properties as best as possible, and conduct experiments that are comparable and repeatable.

Overall, the two dental impression materials were the best performing materials by a significant margin, with the minor difference between the two being, qualitatively, that the heavy body material was observed to adhere slightly better to the aluminum angle stock because of a slightly higher rigidity. The heavy body dental impression material was therefore tested in the SWT at Mach 2 (at a Reynolds number of approximately 13 million per meter) for 2 hr. The test in the SWT resulted in observations of no problems for use in the planned corner flow experiments, and the application of the material in the stainless steel corner was observed to be identical to the application in the aluminum angle stock. In the corner flow experiments, if any problems with adhesion are encountered, the use of a stronger adhesive with the dental impression materials might be investigated.

The radii in the planned tests would benefit from the use of taped or masked edges (similar to the use of tape in painting) which could be removed after curing for a perfect edge. Additionally, in the creation of precise tapered sections for the planned testing, the use of rapid prototyped molds of the tapered shape are necessary, as formation of tapered sections by hand is extremely difficult.

The two dental impression materials also have applications beyond the planned corner flow experiments, as the suitability for use in supersonic flow could allow them to be used to create other shapes, smooth out imperfections on stainless steel models, and create fillets for other experiments.

References

1. Benson, Tom, "Inlet Performance," *Guided Tours of the BGA*, National Aeronautics and Space Administration - Glenn Research Center, 04 Aug. 2009, Web, 26 Nov. 2012, <<http://www.grc.nasa.gov/WWW/k-12/airplane/inleth.html>>.
2. Pritchard, Philip J., Leylegian, John C., "Fox and McDonald's Introduction to Fluid Mechanics," 8th ed. Hoboken: John Wiley & Sons, 2011, Print.
3. Fukuda, Michael K., Hingst, Warren G., Reshotko, Eli, "Control of Shock Wave - Boundary Layer Interactions by Bleed in Supersonic Mixed Compression Inlets," NASA CR-2595, 1975.

4. Anderson, Bernhard H., Tinapple, Jon, Surber, Lewis, "Optimal Control of Shock Wave Turbulent Boundary Layer Interactions Using Micro-Array Actuation," AIAA Paper 2006-3197, June 2006.
5. Blinde, Paul L., Humble, Ray A., Van Oudheusden, Bas W., Scarano, Fulvio, "Effects of micro-ramps on a shock wave/turbulent boundary layer interaction," Shock Waves, December 2009, Vol. 19, Issue 6 (2009), pp. 507-520.
6. Babinsky, H., Li, Y., Ford, C.W. Pitt, "Microramp Control of Supersonic Oblique Shock-Wave/Boundary-Layer Interactions," AIAA Journal, Vol. 47, No. 3 (2009), pp. 668-675.
7. Hirt, Stefanie M., Anderson Bernhard H., "Experimental Investigation of the Application of Microramp Flow Control to an Oblique Shock Interaction," AIAA Paper 2009-919, January 2009.
8. "The Pratt & Whitney J-58 Engine," The 456th Fighter Interceptor Squadron, 10 Feb. 2009, Web, 13 Dec. 2012, <http://www.456fis.org/YF-12A_SR-71_ENGINE.htm>.
9. Hirt, Stefanie M., Chima, Rodrick V., Vyas, Manan A., Wayman, Thomas R., Connors, Timothy R., Reger, Robert W., "Experimental Investigation of a Large-Scale Low-Boom Inlet Concept," AIAA Paper 2011-3796, June 2011.
10. Titchener, Neil, Babinsky, Holger, "Shock Boundary Layer Interaction Flow Control with Micro Vortex Generators," Air Force Research Laboratory, Air Force Office of Scientific Research, United Kingdom, Technical Report 2011-0014, March 2011.
11. Eagle, W. Ethan, Driscoll, James F., Benek, John A., "Experimental Investigation of Corner Flows in Rectangular Supersonic Inlets With 3D Shock-Boundary Layer Effects," AIAA Paper 2011-857, January 2011.
12. Bruce, P.J.K., Babinsky, H., Tartinville, B., Hirsch, C., "Corner Effect and Asymmetry in Transonic Channel Flows," AIAA Journal, Vol. 49, No. 11 (2011), pp. 2382-2392.
13. Bruce, P.J.K., Burton, D.M.F., Titchener, N.A., Babinsky, H., "Corner effect and separation in transonic channel flows," Journal of Fluid Mechanics, Vol. 679, July 2011, pp. 247-262.
14. Vyas, Manan A., Hirt, Stefanie M., Anderson, Bernhard H., "Experimental Investigation of Normal Shock Boundary-Layer Interaction With Hybrid Flow Control," AIAA Paper 2012-0048, January 2012.
15. Baruzzini, Dan, Domel, Neal, Miller, Daniel N., "Addressing Corner Interactions Generated by Oblique Shock-Waves in Unswept Right-Angle Corners and Implications for High-Speed Inlets," AIAA Paper 2012-0275, January 2012.
16. Burton, D.M.F., Babinsky, H., Bruce, P.J.K., "Experimental Investigation into Parameters Governing Corner Interaction for Transonic Shock Wave/Boundary Layer Interactions," AIAA Paper 2010-871, January 2010.
17. Zygo Corporation, "MetroPro Reference Guide OMP-0347K," Rev. K, August 2006, Web, August 2007, <www.zygo.com>.
18. Wheeler, Anthony J., Ganji, Ahmad R., "Introduction to Engineering Experimentation," 3rd ed. New York: Prentice Hall, 2010, Print.

Appendix A.—“Material Samples”

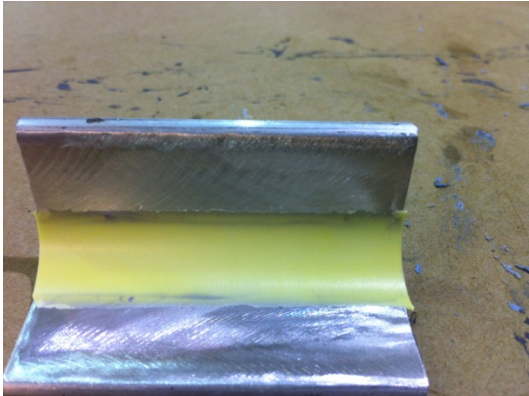


Figure 12.—Heavy body dental impression material.

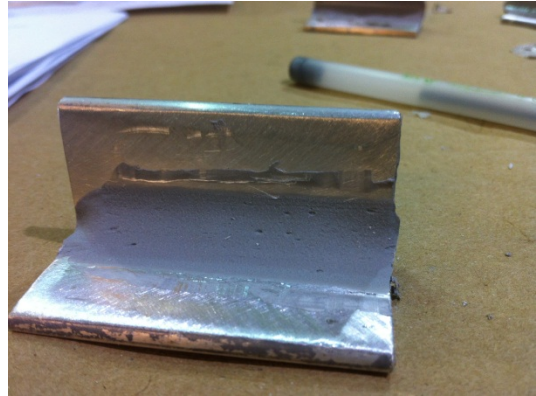


Figure 13.—Polyester filler paste.

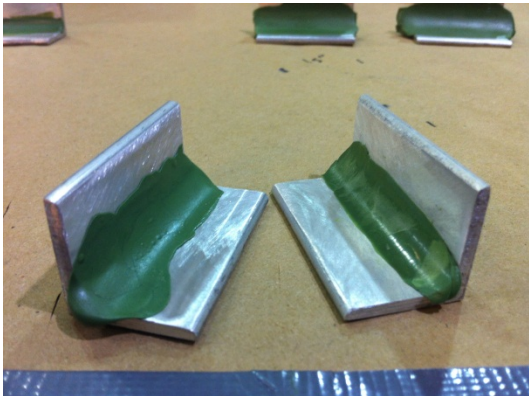


Figure 14.—Basic sculpting epoxy.

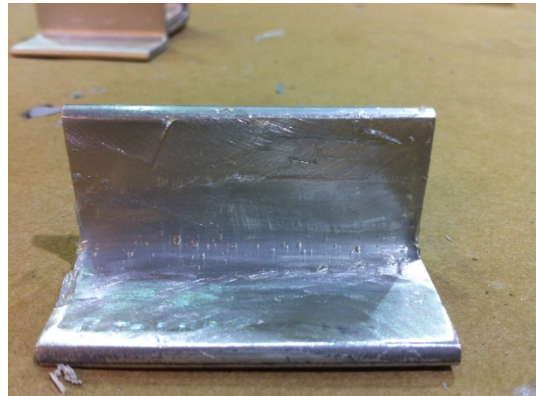


Figure 15.—Resin/solvent based sealant.

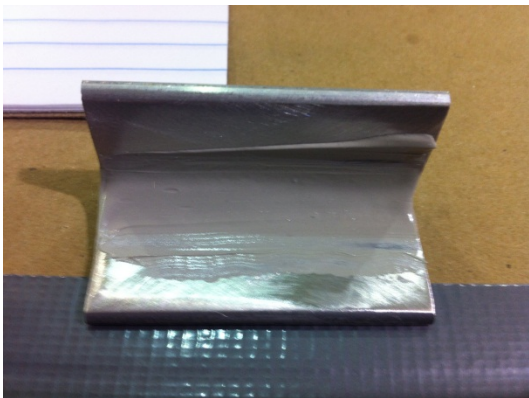


Figure 16.—Polyurethane sealant.



Figure 17.—Silicone adhesive sealant.

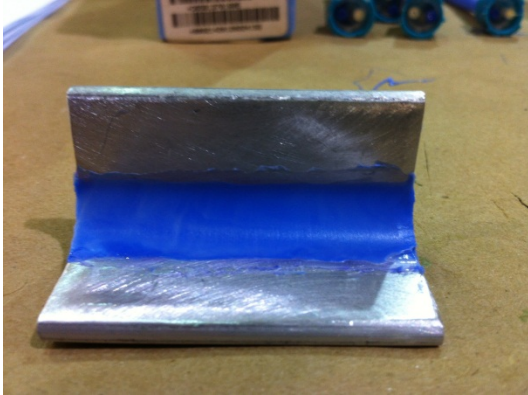


Figure 18.—Regular type dental impression material.



Figure 19.—Spackling paste.

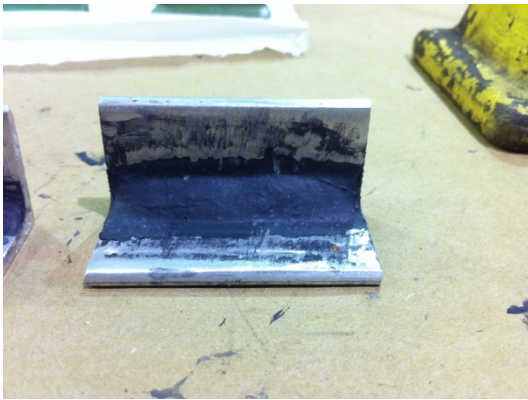


Figure 20.—Silicate cement.



Figure 21.—Vinyl adhesive caulk.

Appendix B.—“Surface Roughness and Eccentricity Data”

TABLE 6.—MATERIALS SORTED BY CHOICE
FOR USE IN THE WIND TUNNEL
AS CORNER FLOW CONTROL

Choice	Material
1	Dental impression (plastic rod)
2	Heavy body dental impression
3	Regular type dental impression
4	Basic epoxy
5	Polyurethane sealant
6	Resin/solvent based sealant
7	Silicone adhesive sealant
8	Spackling paste
9	Vinyl adhesive caulk
10	Silicate cement
11	Polyester filler paste

TABLE 7.—MATERIALS SORTED FROM LOWEST TO
HIGHEST SURFACE ROUGHNESS

Rank	Material	R_a (μm) $\pm 0.020 \mu\text{m}$
1	Heavy body dental impression (plastic rod)	0.2781
2	Regular type dental impression (plastic rod)	0.8790
3	Heavy body dental impression	1.1533
4	Regular type dental impression	1.3310
5	Resin/solvent based sealant	1.8353
6	Polyurethane sealant	1.9473
7	Basic epoxy	1.9873
8	Silicone adhesive	3.1523
9	Polyester filler paste	6.7817
10	Silicate cement	6.9183
11	Spackling paste	7.0660
12	Vinyl adhesive caulk	10.9183

TABLE 8.—MATERIALS SORTED FROM LOWEST TO
HIGHEST AVERAGE ECCENTRICITY

Rank	Material	Average eccentricity
1	Regular type dental impression (plastic rod)	0.0582
2	Heavy body dental impression (plastic rod)	0.1942
3	Regular type dental impression	0.2212
4	Basic epoxy	0.3710
5	Silicone adhesive sealant	0.2605
6	Heavy body dental impression	0.2668
7	Polyurethane sealant	0.6471
8	Vinyl adhesive caulk	0.7349
9	Silicate cement	0.7917
10	Spackling paste	0.8087
11	Resin/solvent based sealant	0.8652
12	Polyester filler paste	0.9587

REPORT DOCUMENTATION PAGE			Form Approved OMB No. 0704-0188		
<p>The public reporting burden for this collection of information is estimated to average 1 hour per response, including the time for reviewing instructions, searching existing data sources, gathering and maintaining the data needed, and completing and reviewing the collection of information. Send comments regarding this burden estimate or any other aspect of this collection of information, including suggestions for reducing this burden, to Department of Defense, Washington Headquarters Services, Directorate for Information Operations and Reports (0704-0188), 1215 Jefferson Davis Highway, Suite 1204, Arlington, VA 22202-4302. Respondents should be aware that notwithstanding any other provision of law, no person shall be subject to any penalty for failing to comply with a collection of information if it does not display a currently valid OMB control number.</p> <p>PLEASE DO NOT RETURN YOUR FORM TO THE ABOVE ADDRESS.</p>					
1. REPORT DATE (DD-MM-YYYY) 01-11-2013		2. REPORT TYPE Technical Memorandum		3. DATES COVERED (From - To)	
4. TITLE AND SUBTITLE Investigation of Materials for Boundary Layer Control in a Supersonic Wind Tunnel			5a. CONTRACT NUMBER		
			5b. GRANT NUMBER		
			5c. PROGRAM ELEMENT NUMBER		
6. AUTHOR(S) Brafladt, Alexander, C.; Lucero, John, M.; Hirt, Stefanie, M.			5d. PROJECT NUMBER		
			5e. TASK NUMBER		
			5f. WORK UNIT NUMBER WBS 794072.02.03.02.01		
7. PERFORMING ORGANIZATION NAME(S) AND ADDRESS(ES) National Aeronautics and Space Administration John H. Glenn Research Center at Lewis Field Cleveland, Ohio 44135-3191			8. PERFORMING ORGANIZATION REPORT NUMBER E-18708		
9. SPONSORING/MONITORING AGENCY NAME(S) AND ADDRESS(ES) National Aeronautics and Space Administration Washington, DC 20546-0001			10. SPONSORING/MONITOR'S ACRONYM(S) NASA		
			11. SPONSORING/MONITORING REPORT NUMBER NASA/TM-2013-217894		
12. DISTRIBUTION/AVAILABILITY STATEMENT Unclassified-Unlimited Subject Categories: 09, 34, and 66 Available electronically at http://www.sti.nasa.gov This publication is available from the NASA Center for AeroSpace Information, 443-757-5802					
13. SUPPLEMENTARY NOTES					
14. ABSTRACT During operation of the NASA Glenn Research Center 15- by 15-Centimeter Supersonic Wind Tunnel (SWT), a significant, undesirable corner flow separation is created by the three-dimensional interaction of the wall and floor boundary layers in the tunnel corners following an oblique-shock/boundary-layer interaction. A method to minimize this effect was conceived by connecting the wall and floor boundary layers with a radius of curvature in the corners. The results and observations of a trade study to determine the effectiveness of candidate materials for creating the radius of curvature in the SWT are presented. The experiments in the study focus on the formation of corner fillets of four different radii of curvature, 6.35 mm (0.25 in.), 9.525 mm (0.375 in.), 12.7 mm (0.5 in.), and 15.875 mm (0.625 in.), based on the observed boundary layer thickness of 11.43 mm (0.45 in.). Tests were performed on ten candidate materials to determine shrinkage, surface roughness, cure time, ease of application and removal, adhesion, eccentricity, formability, and repeatability. Of the ten materials, the four materials which exhibited characteristics most promising for effective use were the heavy body and regular type dental impression materials, the basic sculpting epoxy, and the polyurethane sealant. Of these, the particular material which was most effective, the heavy body dental impression material, was tested in the SWT in Mach 2 flow, and was observed to satisfy all requirements for use in creating the corner fillets in the upcoming experiments on shock-wave/boundary-layer interaction.					
15. SUBJECT TERMS Boundary layer; Corner; Flow control; Material; Radius of curvature; Shock wave; Supersonic Wind Tunnel (SWT)					
16. SECURITY CLASSIFICATION OF:			17. LIMITATION OF ABSTRACT UU	18. NUMBER OF PAGES 24	19a. NAME OF RESPONSIBLE PERSON STI Help Desk (email: help@sti.nasa.gov)
a. REPORT U	b. ABSTRACT U	c. THIS PAGE U			19b. TELEPHONE NUMBER (include area code) 443-757-5802

